Developmental Biology 351 (2011) 200–207

Contents lists available at ScienceDirect

Developmental Biology

journal homepage: www.elsevier.com/developmentalbiology

Evolution of Developmental Control Mechanisms

Proliferating cells in suborbital tissue drive eye migration in flatfish

Baolong Bao [a,*,1], Zhonghe Ke [a,1], Jubin Xing [a,1], Eric Peatman [b], Zhanjiang Liu [a,b], Caixia Xie [a], Bing Xu [a], Junwei Gai [a], Xiaoling Gong [a], Guimei Yang [c], Yan Jiang [a], Wenqiao Tang [a], Daming Ren [c]

[a] The Key Laboratory of Exploration and Utilization of Aquatic Genetic Resources, Shanghai Ocean University, Ministry of Education, Shanghai 201306, PR China
[b] The Fish Molecular Genetics and Biotechnology Laboratory, Department of Fisheries and Allied Aquacultures and Program of Cell and Molecular Biosciences, Aquatic Genomics Unit, Auburn University, Auburn, AL 36849, USA
[c] The State Key Laboratory of Genetic Engineering, Institute of Genetics, Fudan University, Shanghai 200433, PR China

ARTICLE INFO

Article history:
Received for publication 8 September 2010
Revised 14 December 2010
Accepted 18 December 2010
Available online 31 December 2010

Keywords:
Left/right asymmetry
Flatfish
Eye migration
Cell proliferation
Cranial asymmetry
Suborbital tissue

ABSTRACT

The left/right asymmetry of adult flatfishes (Pleuronectiformes) is remarkable given the external body symmetry of the larval fish. The best-known change is the migration of their eyes: one eye migrates from one side to the other. Two extinct primitive pleuronectiformes with incomplete orbital migration have again attracted public attention to the mechanism of eye migration, a subject of speculation and research for over a century. Cranial asymmetry is currently believed to be responsible for eye migration. Contrary to that hypothesis, we show here that the initial migration of the eye is caused by cell proliferation in the suborbital tissue of the blind side and that the twist of frontal bone is dependent on eye migration. The inhibition of cell proliferation in the suborbital area of the blind side by microinjected colchicine was able to prevent eye migration and, thereafter, cranial asymmetry in juvenile *Solea senegalensis* (right sideness, Soleidae), *Cynoglossus semilaevis* (left sideness, Cynoglossidae), and *Paralichthys olivaceus* (left sideness, Paralichthyidae) with a bottom-dwelling lifestyle. Our results correct the current misunderstanding that eye migration is driven by the cranial asymmetry and simplify the explanation for broken left/right eye-symmetry. Our findings should help to focus the search on eye migration-related genes associated with cell proliferation. Finally, a novel model is proposed in this research which provides a reasonable explanation for differences in the migrating eye between, and sometimes within, different species of flatfish and which should aid in our overall understanding of eye migration in the ontogenesis and evolution of Pleuronectiformes.

Introduction

Most vertebrates exhibit a distinct left/right asymmetry of some internal organs, while appearing bilaterally symmetry on the outside. Flatfish (Pleuronectiformes), however, are unusual in their asymmetrical external appearance, and the left/right asymmetry of adult flatfishes is remarkable given the perfect symmetry of the larval fish. Of particular interest in flatfishes is eye-asymmetry (Ahlstrom et al., 1984; Youson, 1988). The eye migration in Pleuronectiformes varies from one species to another and even within the same species such as the "spiny turbot" (Psettodes). Flatfish with eye left/right asymmetry is a type of directional conspicuous asymmetry and is evidently inherited (Palmer, 2004; Babcock, 2005). The genetic mechanism involved in eye migration is uncertain even though it has been the focus of speculation and research for over one century (Brewster, 1987; Traquair, 1865; Giard, 1877; Agassiz, 1879; Willians, 1901; Futch, 1977; Evseenko, 1978; Policansky, 1982). More recently, two adult forms of primitive fossil flatfishes (Amphistium and Heteronectes) with incomplete orbital migration were found by Friedman (2008), linking flatfishes with symmetrical relatives and attracting extensive attention worldwide.

The transformation of symmetrical larvae into asymmetrical juveniles is well documented (Ahlstrom et al., 1984; Youson, 1988; Palmer, 2004; Babcock, 2005; Traquair, 1865; Giard, 1877; Agassiz, 1879; Willians, 1901; Futch, 1977; Evseenko, 1978). Currently, it is widely accepted that cranial asymmetry involving several bones including frontal bone, lateral ethmoid, and pseudomesial bar (in some species) is responsible for eye migration (Brewster, 1987; Wagemans et al., 1998; Okada et al., 2001). If eye migration is caused by cranial asymmetry, its initiation would be expected to occur earlier than initial eye migration. However, only based

Table 1
Metamorphic stages and corresponding days after hatch in *Solea senegalensis*, *Cynoglossus semilaevis*, and *Paralichthys olivaceus*.

Species	Pre-metamorphosis (DAH)	Metamorphosis (DAH)				Rear temperature (°C)
		Stage E	Stage F	Stage G	Stage H	
S. senegalensis	10	14	15	16	17	18
C. semilaevis	15	18	19	19	20	22
P. olivaceus	17	19	21	23	25	20

DAH indicates days after hatch.

* Corresponding author. Fax: +86 21 61900426.
E-mail address: blbao@shou.edu.cn (B. Bao).
[1] These authors contributed equally.

0012-1606/$ – see front matter © 2011 Elsevier Inc. All rights reserved.
doi:10.1016/j.ydbio.2010.12.032

Table 2
Schedule for microinjection of colchicine in *Solea senegalensis*, *Cynoglossus semilaevis*, and *Paralichthys olivaceus*.

Species	Group	No. of injected individuals	Date for injection	No. of survivors	Date for statistics
S. senegalensis	Colchicine injected	82	10, 13 DAH	25	21 DAH
	Control	67	10, 13 DAH	46	21 DAH
C. semilaevis	Colchicine injected	186	15, 20 DAH	19	25 DAH
	Control	100	15, 20 DAH	27	25 DAH
P. olivaceus	Colchicine injected	210	17, 19, 21 DAH	40	30 DAH
	Control	115	17, 19, 21 DAH	95	30 DAH

DAH indicates days after hatch.

on the observation of bone morphological changes, it is difficult to ascertain initial timing difference between eye migration and cranial asymmetry. Moreover, research of Schreiber (2006) has indicated that asymmetrical skull development alone is insufficient for eye migration in Southern flounder (*Paralichthys lethostigma* L.). Dense cell population of fibroblasts ventral to the eye in Atlantic halibut, *Hippoglossus hippoglossus*, was observed by Sæle et al. (2006) and postulated to be related to eye migration. Based on our understanding of the basic physical principles, we proposed a hypothesis that the force generated from the suborbital area should be the most efficient in pushing the eye upwards, and such a force might be generated by hyper-proliferating cells.

Materials and methods

Fish maintenance

Larvae *Solea senegalensis* (Soleidae), *Cynoglossus semilaevis* (Cynoglossidae), and *Paralichthys olivaceus* (Paralichthyidae) were obtained from Dahua Fisheries Farm (Laizhou, Shandong, China), Mingbo Fisheries Farm (Laizhou, Shandong, China), and the Central Experiment Station of Chinese Academy of Fisheries Sciences (Beidaihe, Hebei, China), respectively. Then, larvae were transported to the laboratory of College of Fisheries and Life Science, Shanghai Ocean University, Shanghai, China, and reared according to the references (Dinis et al., 1999; Bao et al., 2005; Liu et al., 2008). Larvae were fed with live brine shrimp (Artemia) nauplii through the end of metamorphosis. The normal metamorphic stages were defined as the following: pre-metamorphosis (the stage prior to the start of eye migration); Stage E (the eye begins to migrate); Stage F (the migrating eye visible from the ocular side); Stage G (the upper edge of the migrating eye beyond the dorsal margin); Stage H (the upper edge of the migrating eye beyond the dorsal mid-line); Stage I (entire migrating eye past the dorsal mid-line) (Minami, 1982). Under this definition, the days after hatch (DAH) corresponding metamorphosis stages were listed in Table 1.

Cytochemical analysis of whole-mount in situ cell proliferation

Larvae were treated with 0.1% 5′-bromodeoxyruidine (BrdU, Sigma-Aldrich, St. Louis, MO) for 8 h, then 20 larvae were fixed in 4% paraformaldehyde (PFA) overnight and stored in methanol at 4 °C after

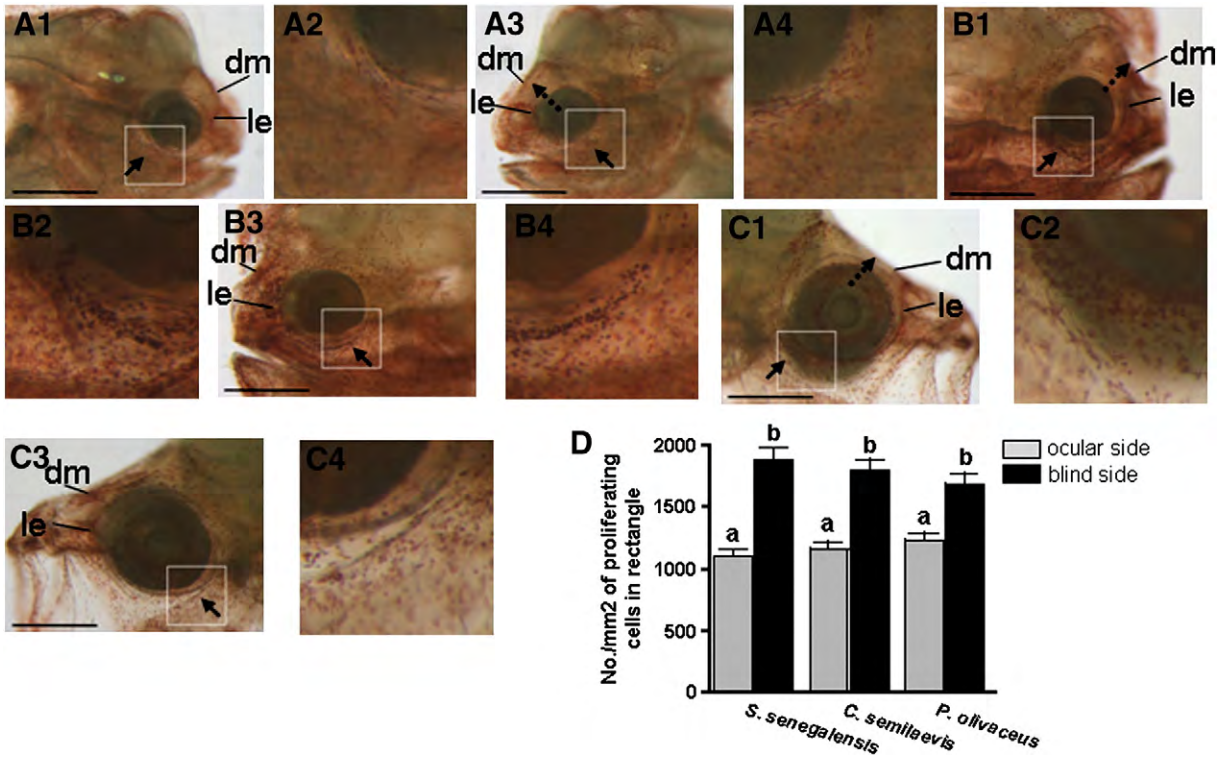

Fig. 1. Left/right asymmetrical distribution of the proliferating cells in suborbital tissue before eye initial movement (pre-metamorphosis stage). The number of proliferating cells can be compared between two rectangle areas (suborbital areas) of both sides of *Solea senegalensis* (right sideness, Soleidae) (panel A), *Cynoglossus semilaevis* (left sideness, Cynoglossidae) (panel B), or *Paralichthys olivaceus* (left sideness, Paralichthyidae) (panel C). Each rectangle area for all three species has the same size. More proliferating cells were found in the suborbital area of blind side than that of ocular side. Proliferating cells in suborbital area of blind side were significantly more than that of ocular side. Panel A, *S. senegalensis*. (A1), ocular view; (A2), enlarged view of rectangle area in A1; (A3), blind view; (A4), enlarged view of rectangle area in A3. Panel B, *C. semilaevis*. (B1), blind view; (B2), enlarged view of rectangle area in B1; (B3), ocular view; (B4), enlarged view of rectangle area in B3. Panel C, *P. olivaceus*. (C1), blind view; (C2) enlarged view of rectangle area in C1; (C3), ocular view; (C4), enlarged view of rectangle area in C3. (D), comparison of proliferating cell number in suborbital area between ocular side and blind side; values are means ± SD, $n = 3$, different letters at top of columns indicate significant differences ($P < 0.05$). dm indicates dorsal mid-line; le, lateral ethmoid. Dash arrow shows movable eye; arrow, signal of cell proliferation. Bar, 500 μm.

anesthetized with 0.1 μg/μl tricaine methanesulfonate (MS 222). The larvae with no BrdU labeling were treated as negative controls. Whole-mount preparations were analyzed for BrdU immunohistochemistry according to techniques developed by Byrd and Brunfes (2001) and modified. Briefly, following fixation, larvae were rinsed in 0.1 M phosphate-buffered saline (PBS), pH 7.4. Then, the fish were bleached with 3% hydrogen peroxide in 25 mM NaOH under strong light and transferred to 2 M HCl at 37 °C for 90 min for DNA denaturation. After neutralization with 0.1 M sodium borate for 20 min, the fish were rinsed 3 times with 0.5% Triton X-100 in PBST for 20 min each. Proteinase K (67 μg/ml in PBST) was used to digest the fish at 37 °C for 30–60 min (depends on the size of fish, smaller fish are more sensitive to proteinase K); then, digestion was terminated by 100 mM glycine for 20 min. The larvae then were rinsed twice with 0.5% Triton X-100 in PBST for 20 min each. Nonspecific binding was blocked by using 5% goat serum, 1% BSA, and 0.5% Triton X-100 in PBST at 37 °C for 90 min. The larvae were incubated with mouse Monoclonal Anti-BrdU antibody (Sigma-Aldrich) at 4 °C overnight. After washing several times with PBST containing 0.5% Triton X-100, the larvae were incubated with HRP conjugated goat anti-mouse secondary antibody (Immunology Consultants Laboratory, Newberg, OR) at 4 °C overnight. Through rinses with PBST and PBS, larvae were placed in 3-amino-9-ethylcarbazole (AEC) (Amresco, Solon, OH) solution until the appropriate staining density was attained. The AEC stock solution was prepared by dissolving 10 mg AEC in 1 ml N,N-dimethylformamide (Amresco). For the actual development, 1 ml of this AEC stock solution was freshly diluted into 30 ml of 0.1 M sodium-acetate buffer (pH 5.0) and mixed with 15 ml H_2O_2. Whole-mount specimens were observed and photographed under a dissecting microscope SZX7 (Olympus, Tokyo, Japan) and documented using Image-Pro Plus 6.0 software (Media Cybernetics, Bethesda, MD). Since BrdU was incorporated into DNA during the synthesis-phase of the cell cycle, the detected signal was only limited in the cell nucleus and hence allows us to count the proliferating cells exactly. Based on the signals on the photograph, the proliferating cells in suborbital areas from each species were counted. Selected specimens were embedded with embedding medium (Leica Instruments, Germany). Eight micrometer frozen tissue sections were cut in the transverse planes to localize precisely signal sites of proliferation and were photographed by the above microscope with Q16242 digital camera (QImaging, Surrey, BC, Canada).

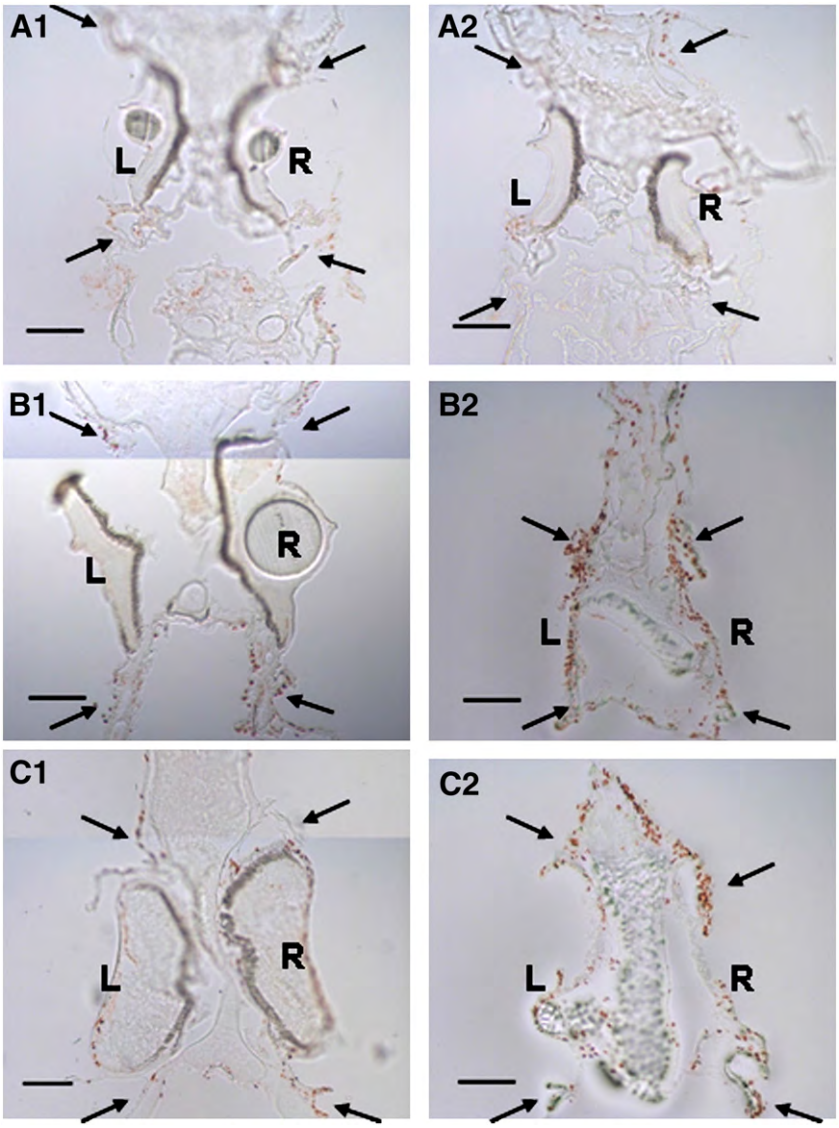

Fig. 2. The signal of cell proliferation locating in the skin of suborbital areas at pre-metamorphosis stage. Panel A, section view across both eyes in *Solea senegalensis*. Cell proliferation in the skin of suborbital area (A1) and along ongoing migration route between two eyes (A2). Panel B, section view across both eyes in *Cynoglossus semilaevis*. Panel C, section view across both eyes in *Paralichthys olivaceus*. Arrow shows signal of cell proliferation. L indicates left side; R, right side; bar, 100 μm.

Microinjection with colchicine

To test the role of cell proliferation in eye migration, colchicine, an inhibitor of cell proliferation, was microinjected into the suborbital area of blind side at several days early before the putative initial eye migration (Table 2). The primary result from pre-test showed that colchicine (Sigma-Aldrich) at concentration of 500 μg/ml could kill the larvae *P. olivaceus* in 36 h. Finally, the concentration of 50 μg/ml colchicine was used in all formal experiments in this research. Appropriate 50 nl of colchicine at 50 μg/ml in 0.75% NaCl solution was injected into the suborbital area of anesthetized larvae. Same amount of 0.75% NaCl solution was injected as control. The injected larvae were reared in 2 L tank with same rearing condition as described above. Detailed information of colchicine injection was listed in Table 2. Several 19 DAH *S. senegalensis*, 25 DAH *C. semilaevis*, and 29 DAH *P. olivaceus* after colchicine injection were treated with 0.1% BrdU for another 8 h for detection of cell proliferation.

Skeletal staining and photography

Larvae and juvenile were fixed in 4% paraformaldehyde for at least 24 h. Alcian blue 8GX (A3157; Amresco) was used for cartilage staining, and alizarin red S (A5533; Amresco) was for bone staining. Detailed staining procedures followed the reference (Gavaia et al., 1999). Samplers were observed under a dissecting microscope SZX7 (Olympus) and documented by using Image-Pro Plus 6.0 software (Media Cybernetics). The scale on each photograph was autogenerated by Image-Pro Plus 6.0 software based on magnification.

Statistics

Significance of difference between two groups was tested by paired *t*-test. SPSS 13.0 (SPSS Inc., Chicago, IL) was used for statistical analysis. Difference was considered significant if $P<0.05$. Data were reported as mean ± SD.

Results

Left/right asymmetrical distribution of the proliferating cells in suborbital tissue before eye initial migration

Using whole-mount *in situ* BrdU detection, we examined cell proliferation during eye migration of three species of flatfish, *S. senegalensis*, *C. semilaevis*, and *P. olivaceus*. At the pre-metamorphosis stage of initial upward eye migration, cell proliferation was found in the suborbital areas on both sides and the dorsal mid-line surface along the head between two eyes (Fig. 1). In *S. senegalensis*, more proliferating cells on the blind side (left side) were found in the suborbital area than that on the ocular side (right side; Fig. 1A). Similar result was observed in *C. semilaevis* (Fig. 1B) and *P. olivaceus* (Fig. 1C). Further analysis showed that these left/right differences in *S. senegalensis*, *C. semilaevis*, and *P. olivaceus* were statistically significant (Fig. 1D, $P<0.05$). In the frontal cartilage, regarded previously as the

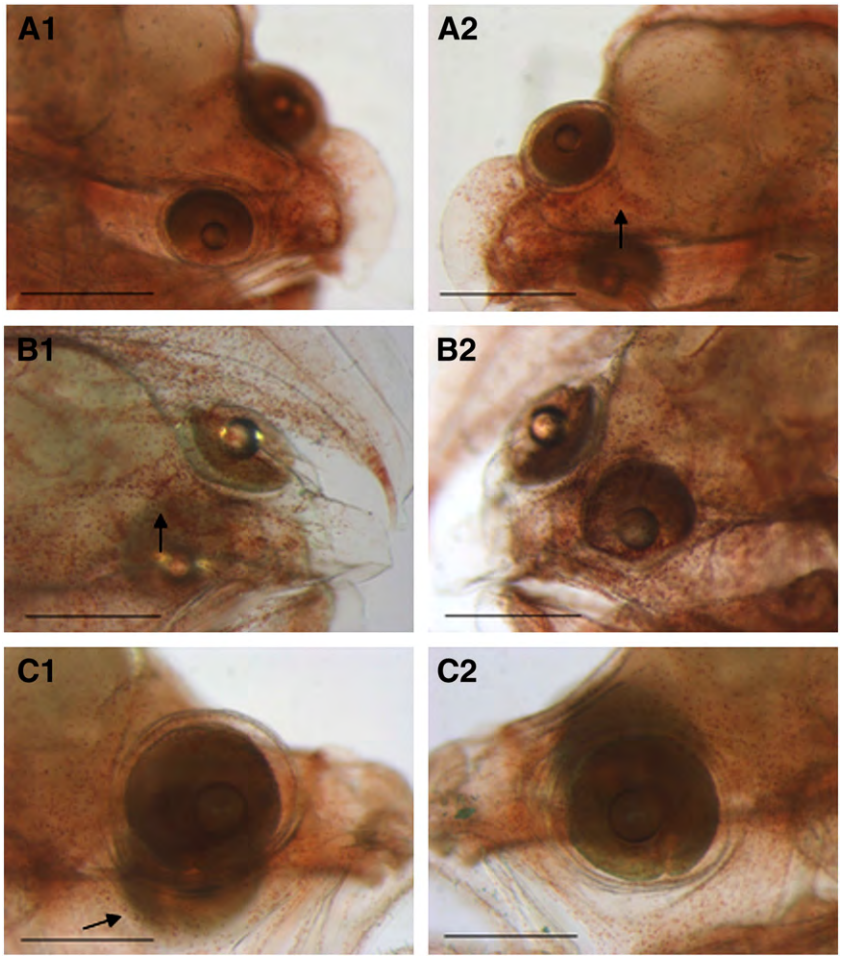

Fig. 3. Cells proliferating in the suborbital tissue at climax of metamorphosis. Panel A, *Solea senegalensis* at 16 DAH. (A1), ocular view; (A2), blind view. Panel B, *Cynoglossus semilaevis* at 20 DAH. (B1), blind view; (B2), ocular view. Panel C, *Paralichthys olivaceus* at 24 DAH. (C1), blind view; (C2), ocular view. More proliferating cells are shown by arrows in the suborbital area of migrating eye. Bar, 500 μm.

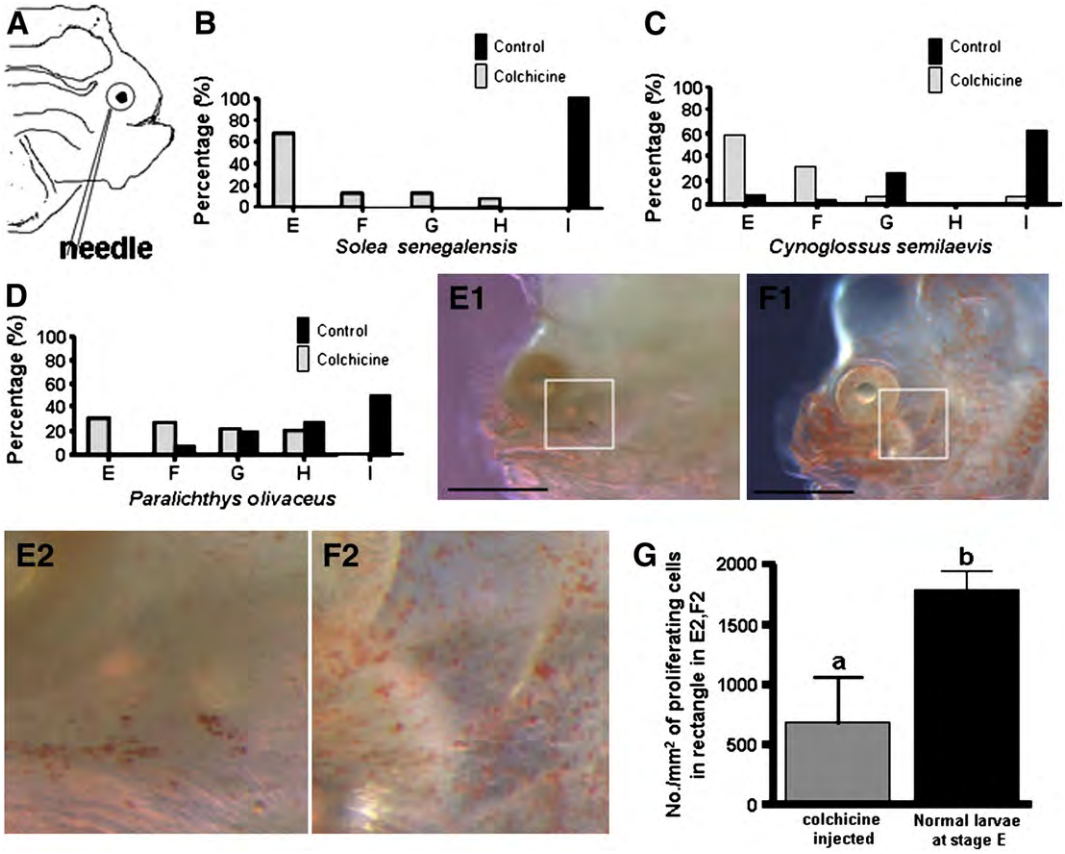

Fig. 4. Eye migration stopped by colchicine through microinjecting into the suborbital area of blind side. (A), the suborbital area of blind side where colchicine was microinjected. (B), the percentage of various *Solea senegalensis* with eye stopped in different locations at age of 21 DAH. (C), the percentage of various *Cynoglossus semilaevis* with eye stopped in different locations at age of 25 DAH. (D), the percentage of various *Paralichthys olivaceus* with eye stopped in different location at age of 30 DAH. Gray column, injected with colchicine; black column, injected with 0.75% NaCl solution (control). Metamorphic stages shown with E (the eye begins to migrate), F (the migrating eye visible from the ocular side), G (the upper edge of the migrating eye beyond the dorsal margin), H (the upper edge of the migrating eye beyond the dorsal mid-line), and I (entire migrating eye past the dorsal mid-line) on abscissa axis. (E1), proliferating cells of 19 DAH *Solea senegalensis* after colchicine microinjected into suborbital area of blind side; rectangle shows suborbital area. (E2), enlarged view of rectangle area in E1. (F1), proliferating cells of normal larvae at stage E (the eye begins to migrate); rectangle shows suborbital area. (F2), enlarged view of rectangle area in F1. (G), proliferating cells in the suborbital area of blind side in *S. senegalensis* injected with colchicine were significantly less than that in normal larvae at stage E; values are means ± SD, $n = 3$, different letters at top of columns indicate significant differences ($P<0.05$). Bar, 500 μm.

source of the original force initiating eye migration, there was no cell proliferation signal found. Whereas in the lateral ethmoid, which was thought previously to push eye migration at later metamorphic stage through asymmetrical enlargement on both sides, there existed a strong signal of cell proliferation (Fig. 1A1, A3, B1, B3, C1, C3). The signal of cell proliferation located in the skin of suborbital area and along the head between two eyes in *S. senegalensis*, *C. semilaevis*, and *P. olivaceus* (Fig. 2). The phenotype of proliferating cell could not be discerned in the frozen tissue sections in this research. After initiation of eye migration, the cells in suborbital tissue on both sides and the

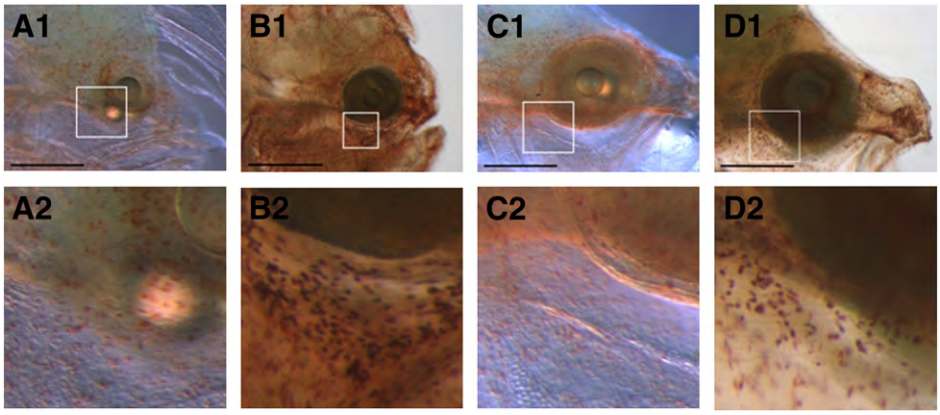

Fig. 5. Cell proliferation inhibited by colchicine through microinjecting into the suborbital area of blind side in *Cynoglossus semilaevis* and *Paralichthys olivaceus*. Panel A, proliferating cells of 25 DAH *C. semilaevis* after colchicine microinjected into suborbital area of blind side. Rectangle shows the suborbital area (A1) and its enlarged view (A2). Panel B, proliferating cells of normal larvae *C. semilaevis* at stage E (the eye begins to migrate). Rectangle shows suborbital area of blind side (B1) and its enlarged view (B2). Panel C, proliferating cells of 29 DAH *P. olivaceus* after colchicine microinjected into suborbital area of blind side. Rectangle shows the suborbital area (C1) and its enlarged view (C2). Panel D, proliferating cells of normal larvae *P. olivaceus* at stage E. Rectangle shows the suborbital area of blind side (D1) and its enlarged view (D2). Bar, 500 μm.

dorsal surface along the head between the two eyes continue proliferating in *S. senegalensis*, *C. semilaevis*, and *P. olivaceus* (Fig. 3).

Eye migration stopped by the inhibitor of cell proliferation microinjected into the suborbital area of blind side

To determine the role of cell proliferation of suborbital tissue in initial eye migration, colchicine, a widely used inhibitor of cell proliferation, was microinjected two to three times into the suborbital area of the blind side four, three, or two days before initial eye migration in *S. senegalensis*, *C. semilaevis*, or *P. olivaceus*, respectively (Table 2, Fig. 4A). Eye migration could be stopped by injected colchicine. In *S. senegalensis*, while the eye on blind side in all larvae without colchicine injection successfully migrated past the dorsal mid-line (Stage I, 21 DAH), there were no larvae with eye migration past the dorsal mid-line (Stage I) in the colchicine microinjected group, and 17 (68%) individuals were at stage E with no observable movement of the eye on blind (left) side (Fig. 4B). Similar results were observed in *C. semilaevis* (Fig. 4C) and *P. olivaceus* (Fig. 4D). Moreover, while eye migration was partially or completely inhibited by microinjection of colchicine in the suborbital area of the blind side, all larvae went through metamorphosis successfully and developed into juveniles with a bottom-dwelling lifestyle with the exception of abnormal eye location. This result suggests that inhibition of eye migration was specific to interference with proliferating cells in suborbital tissue and not due to a general developmental disruption caused by colchicine injection. The cell proliferation in the suborbital area of the blind side was evidently inhibited by microinjected colchicine. Since colchicine inhibited cell mitosis through inhibiting microtubule polymerization by binding to tubulin, not through inhibiting DNA synthesis, the signal of cell proliferation from BrdU labeling still could be detected. However, the number of proliferating cells did not increase. Compared with normal larvae at stage E (the eye begins to migrate), less proliferating cells were found in the suborbital area of blind side in *S. senegalensis* injected with colchicine (Fig. 4E, F). Further analysis showed that the difference was statistically significant (Fig. 4G, $P<0.05$). Similar inhibition of cell proliferation by microinjected colchicine in *C. semilaevis* and *P. olivaceus* are shown in Fig. 5. Representative individuals of *S. senegalensis*, *C. semilaevis*, and *P. olivaceus* with eye migration blocked completely by microinjected colchicine are shown in Fig. 6. Representative individuals with incomplete eye migration caused by microinjected colchicine are shown in Fig. 7.

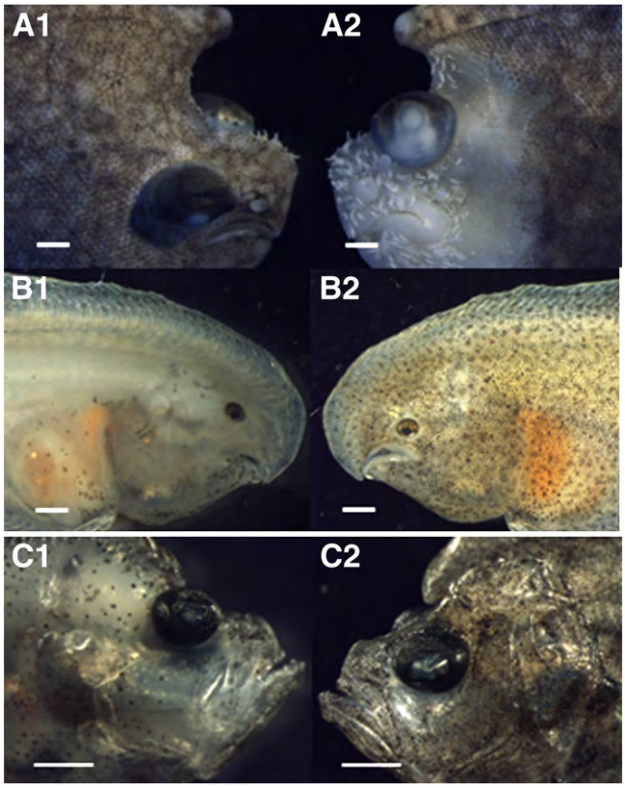

Fig. 7. Representative individuals with incomplete eye migration caused by microinjected colchicine. Panel A, *Solea senegalensis*. (A1), ocular view; (A2), blind view. Panel B, *Cynoglossus semilaevis*. (B1), blind view; (B2), ocular view. Panel C, *Paralichthys olivaceus*. (C1), blind view; (C2), ocular view. Bars in panels A and B, 1 mm; bars in panel C, 0.5 mm.

Twist of frontal bones depending on eye migration

The juvenile with symmetrical eyes resulting from colchicine injection in this research provided an opportunity to determine the

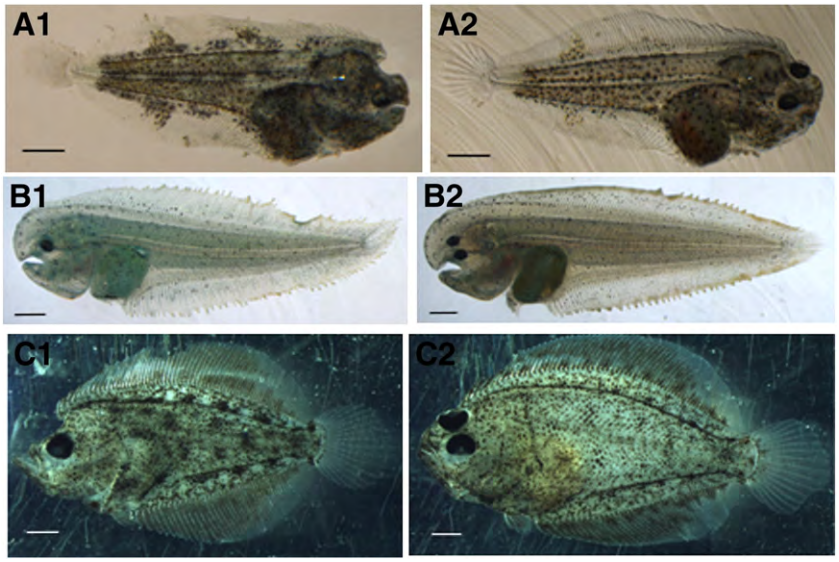

Fig. 6. Representative individuals with eye migration caused by microinjected colchicine. Panel A, eye-symmetry individual of *Solea senegalensis* resulting from microinjected colchicine (A1) and normal eye-asymmetry individual of control group (A2). Panel B, eye-symmetry individual of *Cynoglossus semilaevis* resulting from microinjected colchicine (B1) and normal eye-asymmetry individual of control group (B2). Panel C, eye-symmetry individual of *Paralichthys olivaceus* resulting from microinjected colchicine (C1) and normal eye-asymmetry individual of control group (C2). Bar, 500 μm.

chronological sequence of eye migration and cranial asymmetry. In these flatfishes with symmetrical eyes, the skull kept left/right symmetry (Fig. 8). The twist of frontal cartilage was not observed in the juvenile *S. senegalensis* with symmetrical eyes. The lateral ethmoids on both sides were the similar size (Fig. 8A). Similar development of skull bones was observed in colchicine-treated *C. semilaevis* and *P. olivaceus* with symmetrical eyes (Fig. 8B, C). The observation provided here indicates that cranial asymmetry should depend on the eye migration in normal metamorphosing flatfish.

Discussion

What kind of tissue drives eye migration during metamorphosis is one of the most important issues in better understanding the genetic mechanism behind eye-asymmetry in flatfish. Sæle et al. (2006) first time observed the dense cell population of fibroblasts in the suborbital tissue in *H. hippoglossus* and postulated to be related to eye migration. In this study, we observed the proliferating cells in the suborbital tissue of *S. senegalensis*, *C. semilaevis*, and *P. olivaceus*, suggesting that the proliferating cells might be fibroblast within the suborbital connective tissue as observed in *H. hippoglossus* by Sæle et al. (2006). Moreover, the inhibition of this proliferation with colchicine provides strong evidence that the initial migration of the eye was caused by cell proliferation in the suborbital tissue of the blind side in three different species from families of Pleuronectiformes. In addition, the result in this study showed that the twist of frontal bone, which was thought to be primary reason for eye migration, is dependent on eye migration. It is also the first time in the world to produce eye-symmetrical or incomplete orbital migration juvenile *S. senegalensis*, *C. semilaevis*, and *P. olivaceus* with a bottom-dwelling lifestyle. Based on all the findings in this study, we propose a novel model here to explain eye migration in flatfish (Fig. 9). Before eye migration initiated, the cells located in suborbital tissue (skin) and along the route of ongoing eye migration begin to proliferate (Fig. 9A). More proliferating cells exist in the suborbital tissue of the blind side than that of the ocular side. Left/right asymmetrical distribution of proliferating cells in suborbital tissue may correspond to "stronger" and "feeble" eye identified in an early hypothesis proposed by Giard (1877) in which he suggested that one eye was "stronger" causing it to rotate towards the "feeble" eye. The presence of uneven amount of proliferating cells exerting uneven pressure on two eyes could explain why the migrating eye differs between, and even within, species of flatfish. Generally, only one of the eyes will be able to be pushed upwards by overcrowded proliferating cells in the suborbital tissue. Once the movable eye receives enough pushing force from proliferating cells in its suborbital area to overcome the main counteracting force from the other eye, it starts migrating upwards (Fig. 9A). During migration, the migrating eye receives an additional pushing force from more proliferating cells in its enlarging suborbital area. Meanwhile, the counteracting force is becoming larger and larger as the two eyes become closer and closer (Fig. 9B). When the migrating eye reaches the place where pushing and counteracting forces are equalized, it finally stops migration (Fig. 9C). During the process of eye migration, once the eye starts migrating upwards, the cartilage of the skull closest to the route of the migrating eye (frontal cartilage and/or supraorbital cartilage in some species) begins facing the pushing force from the migrating eye and, in response, begins twisting towards another side.

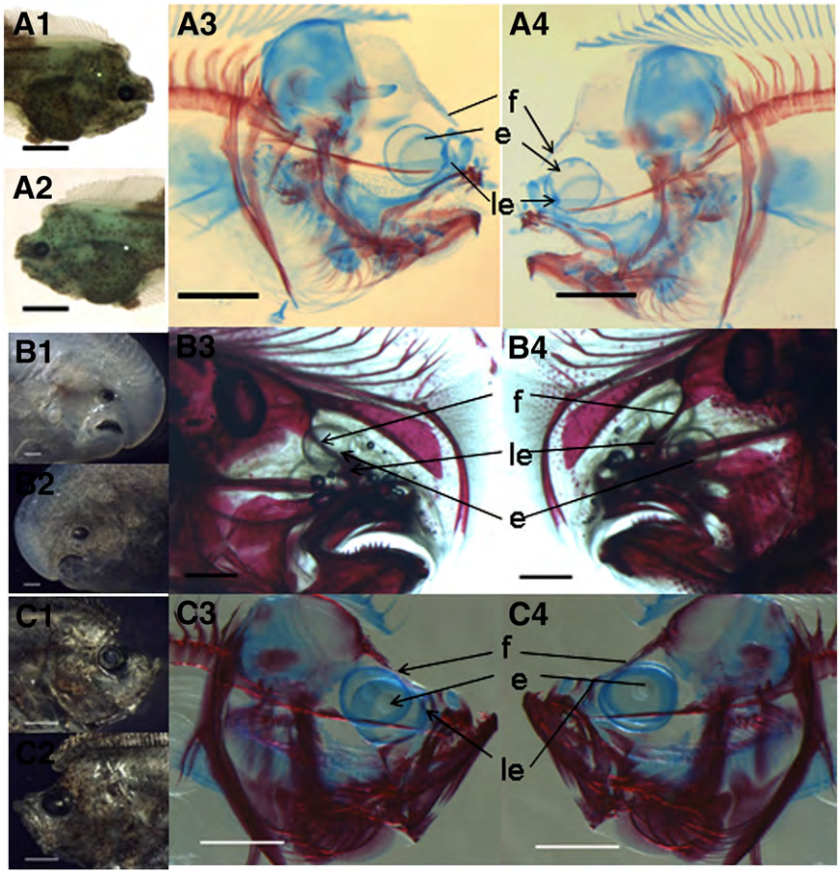

Fig. 8. Left/right symmetry of skull in the colchicine-treated flatfish with symmetrical eyes. There was no twist found in frontal bones (f), and lateral ethmoids (le) on both sides of head were similar size in the juvenile with symmetrical eyes. Panel A, 21 DAH symmetrical-eyed *Solea senegalensis* resulting from injected colchicine. (A1), ocular view; (A2), blind view; (A3), ocular view of skull; (A4), blind view of skull. Panel B, 60 DAH symmetrical-eyed *Cynoglossus semilaevis* resulting from colchicine. (B1), blind view; (B2), ocular view; (B3), blind view of skull; (B4), ocular view of skull. Panel C, 38 DAH symmetrical-eyed *Paralichthys olivaceus* resulting from colchicine. (C1), blind view; (C2), ocular view; (C3), blind view of skull; (C4), ocular view of skull. Calcified bone is red and cartilage is blue. e indicates eye; f, frontal cartilage/bone; le, lateral ethmoid. Arrow shows the bone on the blind side. Line shows the bone on the ocular side. Bars in A3 and A4, 0.5 mm; bars in others, 1.0 mm.

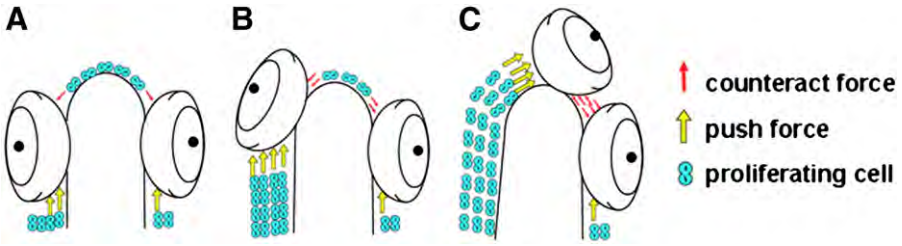

Fig. 9. Schematic drawing to explain eye migration in flatfish. (A), Before eye migration initiated, cells located in the suborbital area and along the route of ongoing eye migration begin proliferating. Uneven amounts of proliferating cells exist in the left and right suborbital tissue. Once the eye receives sufficient pushing force from proliferating cells in its suborbital tissue to overcome the main counteracting force from the other eye, along the route of ongoing eye migration, it begins migrating upwards. Once the eye begins migrating upwards, the cartilage of skull closest to the route of migrating eye begins facing the pressing force from the migrating eye and starts twisting towards the other side. (B), As it migrates along the route between two eyes, the migrating eye gets more pushing force from additional proliferating cells in its enlarging suborbital area. Meanwhile, the counteracting force grows larger as the two eyes become closer. (C), When the migrating eye reaches the place wherein pushing and counteracting force are balanced, it finally stops migration.

Moreover, the lateral ethmoid on the blind side will enlarge more quickly than that on the ocular side because of the additional space left by the migrating eye.

Based on the above model, eye migration in Psettodes that varies from one species to another, and within the same species, and various observed natural mutant flatfish with different eye locations, such as reversed-eye, symmetrical eyes, and both eyes on the top of the head (Schreiber, 2006; Wagemans et al., 1998), are easily understandable. Mutant forms may be the result of abnormal competition between both sides of suborbital areas in the form of cell proliferation.

Our results presented in this study suggest that eye migration is caused by cell proliferation in suborbital tissue and correct the misunderstanding that eye migration is driven by the cranial asymmetry. These findings are important to simplify the explanation for broken left/right symmetry of eyes and will be of great help in identifying eye migration-related genes associated with cell proliferation. Obviously, the proposed model in this research will help us to understand eye migration in the ontogenesis and evolution of Pleuronectiformes.

Acknowledgments

The authors thank Dr. Chenhong Li, University of Nebraska-Lincoln, and Dr. Palmer, A.R. of University of Alberta-Edmonton, for helpful comments on early drafts. This work was supported by National Natural Science Foundation of China 30771668 and 31072201, National Education Commission of China 06ZZ65, and the Key Discipline funding Y1101, Marine Biology funding J50701, Hydrobiology funding S30701, and Marine Advanced Technology Platform funding 6870305 by the Leading Academic Discipline Project of Shanghai Municipal Education Commission, China.

References

Agassiz, A., 1879. On the young stages of bony fishes. Proc. Amer. Acad. Arts Sci. 1, 1–25.
Ahlstrom, E.H., Amaoka, K., Hensley, D.A., Moser, H.G., Sumida, B.Y., 1984. In: Moser, H.G., et al. (Ed.), Ontogeny and Systematics of Fishes. Allen, Lawrence, Kansas, pp. 640–670.
Babcock, L.E., 2005. Asymmetry in the fossil record. Eur. Rev. 13, 135–143.
Bao, B., Yang, G., Liu, Z., Li, S., Wang, Z., Ren, D., 2005. Isolation of SFRS3 gene and its differential expression during metamorphosis involving eye migration of Japanese flounder *Paralichthys olivaceus*. Biochi. Biophy. Acta 1725, 64–70.
Brewster, B., 1987. Eye migration and cranial development during flatfish metamorphosis: a reappraisal (Teleostei: Pleuronectiformes). J. Fish Biol. 31, 805–834.
Byrd, C.A., Brunfes, P.C., 2001. Neurogenesis in the olfactory bulb of adult zebrafish. Neruoscience 105, 793–801.
Dinis, M.T., Ribeiro, L., Soares, F., Sarasquete, C., 1999. A review on the cultivation potential of *Solea senegalensis* in Spain and Portugal. Aquaculture 176, 27–38.
Evseenko, S.A., 1978. Some data on metamorphosis of larvae of the genus Bothus (Pisces, Bothidae) from the Caribbean Sea. Zool. Zh. 57, 1040–1047.
Friedman, M., 2008. The evolutionary origin of flatfish asymmetry. Nature 454, 209–212.
Futch, C.R., 1977. Larvae of *Trichopsetta ventralis* (Pisces: Bothidae), with comments on intergeneric relationships within the Bothidae. Bull. Mar. Sci. 27, 740–757.
Gavaia, P.J., Sarasquete, C., Cancela, M.L., 1999. Detection of mineralized structures in early stages of development of marine Teleostei using a modified alcian blue-alizarin red double staining technique for bone and cartilage. Biotech. Histochem. 75, 79–84.
Giard, A., 1877. Le development des Pleuronectes. Rev. Sci. Nat. 6, 133–139.
Liu, F., Ai, Q., Mai, K., Tan, B., Ma, H., Xu, W., Zhang, W., LiuFu, Z., 2008. Effects of dietary binders on survival and growth performance of postlarval tongue sole, *Cynoglossus semilaevis* (Günther). J. World Aquac. Soc. 39, 500–509.
Minami, T., 1982. The early life history of a flounder *Paralichthys olivaceus*. Bull. Jpn Soc. Sci. Fish. 48, 1581–1588.
Okada, N., Takagi, Y., Seikai, T., Tanaka, M., Tagawa, M., 2001. Asymmetrical development of bones and soft tissues during eye migration of metamorphosing Japanese flounder *Paralichthys olivaceus*. Cell Tissue Res. 304, 59–66.
Palmer, A.R., 2004. Symmetry breaking and the evolution of development. Science 306, 828–833.
Policansky, D., 1982. The asymmetry of flounders. Sci. Am. 246, 116–122.
Sæle, Ø., Silva, N., Pittman, K., 2006. Post-embryonic remodelling of neurocranial elements: a comparative study of normal versus abnormal eye migration in a flatfish, the Atlantic halibut. J. Anat. 209, 31–41.
Schreiber, A.M., 2006. Asymmetric craniofacial remodeling and lateralized behavior in larval flatfish. J. Exp. Biol. 209, 610–621.
Traquair, R.H., 1865. On the asymmetry of the Pleuronectidae, as elucidated by an examination of the skeleton in the turbot, halibut, and plaice. Trans. Linn. Soc. Lond 25, 263–296.
Wagemans, F., Focant, B., Vandewalle, P., 1998. Early development of the cephalic skeleton in the turbot. J. Fish Biol. 52, 166–204.
Willians, S.R., 1901. The changes in the facial cartilaginous skeleton of the flatfish, *Pseudopleuronectes americanus* (a dextral fish) and *Bothus maculatus* (sinistral). Sci. New Ser. 13, 378–379.
Youson, J.H., 1988. In: Hoar, W.S., Randall, D.J. (Eds.), Fish Physiology, 11B. Academic Press, San Diego, pp. 135–196.